

# Characterization and Modeling of 3-D Vibration Modes of a Micromachined U-Shaped Cantilever

John Ojur Dennis, Waddah Abdelbagi Talha, Nor Hisham B Hamid

Department of Electrical and Electronic Engineering  
Universiti Teknologi PETRONAS

Bandar Sri Iskandar, 31750 Tronoh, Perak, Malaysia

Email: [ojur100@yahoo.com](mailto:ojur100@yahoo.com) , [waddah\\_jabor1@yahoo.com](mailto:waddah_jabor1@yahoo.com)

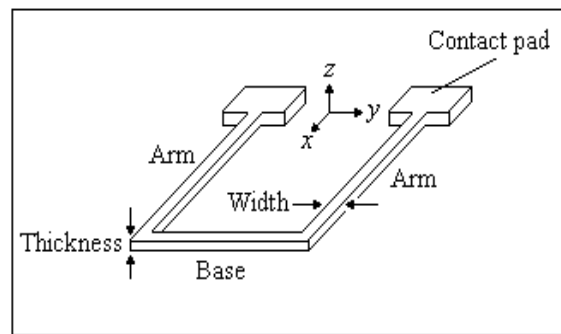
**Abstract-** The present work explores the potential applicability of the Lorentz force actuation of a micromachined U-shaped cantilever device for 3-D vector magnetic field measurements in a broad range of frequencies. The structures simulated are made entirely from aluminum and designed using CMOS fabrication technology and bulk micromachining in CoventorWare simulation environment. Analytical models describing 3-D cantilever vibration modes that are actuated by the Lorentz force and their verification by simulation is discussed. Results show that the resonant frequencies for mode 1 and 2 increase with increasing thickness of the cantilever while it is independent of the thickness for mode 3. On the other hand the resonant frequency for mode 3 increases with increasing width of the cantilever while it is independent of width for mode 1 and 2. It is also observed that the displacement of the cantilever for identical applied Lorentz force is highest, indicated highest sensitivity, for mode 1 and lowest for mode 3.

## I. INTRODUCTION

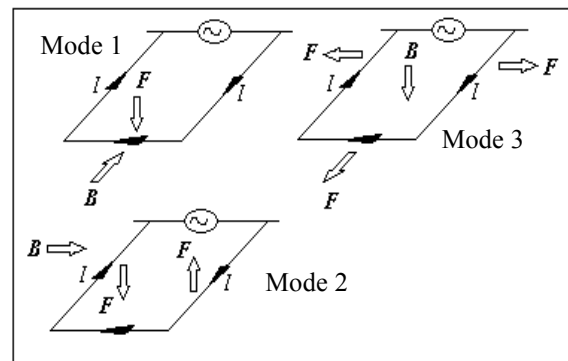
The Lorentz force is a well known physical law that is apparently not widely applied in various types of micromachined sensors and actuators but promises to have numerous potential engineering applications. The elastic properties of micromachined thin-films of metals can be used in 3-D Lorentz force actuation of arbitrary shapes. A micromachined U-shaped cantilever is one of such devices that offer possibilities for actuation and sensing applications. The response of the cantilever can be used to detect the magnitude and direction of an external magnetic field by using the piezoresistive [1, 2] or optical [3] technology. The present work explores the potential applicability of the Lorentz force actuation of a micromachined U-shaped cantilever device for 3-D measurement of magnetic fields in a broad range of frequencies. The structures discussed are made entirely of aluminum because they must be conductive, low cost and CMOS compatible.

Fig. 1(a) shows the structure of a U-shaped cantilever. The Lorentz force,  $F$ , due to a static external magnetic field  $B$  acting on an ac current through the cantilever excites three vibration modes depending on the direction of the magnetic field as shown in Fig. 1 (b). Mode 1 is characterized by the vibrations of the cantilever base in the  $z$ -direction. The external magnetic field is perpendicular to the base of the cantilever and parallel or antiparallel with the current in the arms and therefore no force acts on the arms. To generate

mode 2, on the other hand, the external magnetic field is oriented parallel to the base and perpendicular to the arms. Lorentz forces, therefore, act on the two arms of the U-shaped cantilever in opposite directions along the  $z$ -axis. The Lorentz force in this situation does not act on the base. In mode 3, the external magnetic field is perpendicular to the current in all parts of the cantilever and the Lorentz forces on the base and arms will be directed either inwards or outwards with the arms vibrating in the  $y$ -direction while the base vibrates in the  $x$ -direction but are all in phase with each other. These three modes of vibration provide a possibility for the measurement of the magnitude and direction of magnetic fields in three dimensions (3-D).



(a)



(b)

Fig. 1: (a) Schematic diagram of a U-shaped cantilever and (b) Lorentz forces acting on the base and arms when  $B$  is in the  $x, y$  or  $z$  directions

## II. THEORETICAL MODELING

The Lorentz force is generated when a conductor carrying a direct or alternating electrical current is placed in a static or changing magnetic field. Each of the moving charges in the conductor experiences the Lorentz force, and together they produce a macroscopic force on the conductor given by

$$F_L = IBl \quad (1)$$

where  $F_L$  is the Lorentz force,  $I$  electric current in the conductor,  $B$  is external magnetic field, and  $l$  is the length of the portion of the conductor perpendicular to the external magnetic field.

The three flexural vibration modes of a U-shaped cantilever under the influence of the Lorentz force may be categorized into a symmetrical mode (mode 1) and two antisymmetrical modes (mode 2 and 3). Assuming that the flexural vibrations of the cantilever are small compared to its dimensions (and therefore the effect of shear deformation and rotary inertia are negligible) it's oscillations can be described by the classical Euler-Bernoulli beam dynamics theory leading to a set of three (one for each cantilever arm and one for the cantilever base) coupled 4th-order partial differential equations given by [4]

$$\frac{\partial}{\partial \zeta_i^2} \left( EI_i \frac{\partial^2 \psi_i}{\partial \zeta_i^2} \right) - \left( F_i - \bar{m}_i \frac{\partial^2 \psi_i}{\partial t^2} \right) = 0 \quad (2)$$

where  $E$  is Young's modulus,  $I$  moment of inertia,  $\zeta_i$  spatial coordinate along the cantilever ( $\zeta_{1,2} = x$  and  $\zeta_3 = y$ ),  $i = 1, 2$  and 3 for modes 1, 2 and 3 respectively,  $f_i$  is the applied force,  $\bar{m}_i$  the effective mass,  $t$  is the time, and  $\psi_i(\zeta_i, t)$  is the time dependant transverse deflection.

The moment of inertia,  $I$ , for a single rectangular cantilever of thickness  $h$  and width  $w$  is given by (3). This expression is used for the three vibration modes with the values assigned for the parameters  $h$  and  $w$  depending on the vibration mode selected.

$$I = \frac{1}{12} h^3 w \quad (3)$$

and the stiffness ( $k$ ) for a single cantilever is give by

$$k = \frac{3EI}{l^3} = \frac{Eh^3 w}{4l^3} \quad (4)$$

where  $l$  is the length of the cantilever.

To analyze the flexural vibrations of the U-shaped structure in mode 1, we assume that the two arms of the cantilever are identical. The U-shaped cantilever in mode 1 is therefore equivalent to two regular single cantilevers with half the mass of the base placed at its tip as shown in Fig. 2 (a) [5].

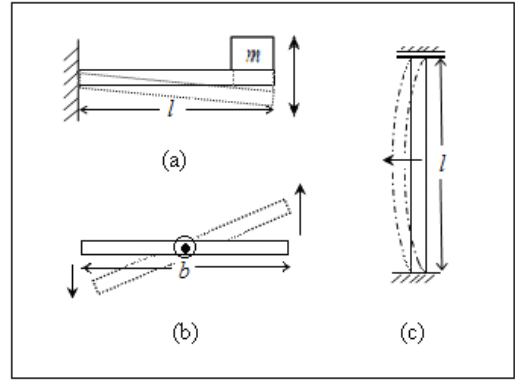


Fig. 2: Model for mechanical vibration of a U-shaped cantilever in (a) mode 1, (b) mode 2 and (c) mode 3 [5].

The stiffness ( $k$ ) for a single cantilever is consequently multiplied by 2 for the mode 1 vibration to take care of the two arms, each supporting half the mass of base, to give

$$k = \frac{6EI}{l^3} = \frac{Eh^3 w}{2l^3}, \quad (5)$$

and the resonant frequency ( $f_0$ ) is determined from

$$f_0 = \frac{1}{2\pi} \sqrt{\frac{k}{m_{eff}}} = \frac{1}{2\pi} \sqrt{\frac{Eh^2}{2\rho l^3 (b/2 + l)}} \quad (6)$$

where  $m_{eff}$  is the effective mass given by the sum of mass of half base,  $m_b/2 = \rho bhw/2$  and mass of arm,  $m_{arm} = \rho bhw l$  to give  $m_{eff} = \rho wh (b/2 + l)$  and  $b$  is the length of base

Fig. 2 (b) is considered for analyzing the antisymmetrical flexural vibration mode (mode 2) of the U-shaped structure. During the vibrations in mode 2, the base pivots around a point of rest located at the centre of the base. Half of the base is therefore replaced by a uniform cantilever supported at the midpoint of the base and the arms are replaced by a lumped mass  $m = \rho lhw$ , where  $l$  is length of the arms. The total effective mass,  $m_{eff}$ , will then be  $\rho wh (b/2 + l)$ .  $k$  is calculated using (4) but replacing the length  $l$  by half of the length of base  $b/2$ . The base then moves with a stiffness constant given by  $k/2$  since there are two forces acting in opposite directions on the base. The modified equation becomes

$$k = \frac{12EI}{b^3} = \frac{Eh^3 w}{b^3}, \quad (7)$$

and the resonant frequency is now

$$f_0 = \frac{1}{2\pi} \sqrt{\frac{k}{m_{eff}}} = \frac{1}{2\pi} \sqrt{\frac{Eh^2}{\rho b^3 (b/2 + l)}} \quad (8)$$

Fig. 2 (c) shows the one-dimensional model for mode 3. Unlike mode 1 and 2, the width of the cantilever in mode 3 becomes its thickness and the thickness becomes its width.

The base now moves slightly since the mechanical force on the base is assumed to be slightly greater than the Lorentz force in the opposite direction. The theoretical value of  $k$  for mode 3 can be estimated from (4) by substituting half the length of cantilever arms ( $l/2$ ) and multiplying by 2 for the whole length since the arms will act like two cantilevers coupled together with one of them becoming the mass for the other. We then obtain

$$k = \frac{48EI}{l^3}. \quad (9)$$

This value of  $k$  is multiplied by a factor of 5 that is assumed in this study to take care of the stiffness due to the moving base and the other arm. Using the new value obtained for  $k$  and taking the effective mass to be the mass of one arm  $m_{\text{eff}} = \rho h w l$  gives for the resonant frequency

$$f_0 = \frac{1}{2\pi} \sqrt{\frac{240EI}{\rho h w l^4}} = \frac{1}{2\pi} \sqrt{\frac{20Ew^2}{\rho l^4}}. \quad (10)$$

We observe that the theoretically derived resonant frequencies in equations 6, 8 and 10 are independent of the cantilever width for modes 1 and 2 while it is independent of the thickness for mode 3. The theoretically calculated values for the resonant frequencies are compared with the values obtained from simulation.

### III. METHODOLOGY

CoventorWare simulation software is used in this study to design micromachined U-shaped cantilevers and perform finite element simulations. CMOS fabrication technology and bulk micromachining is adopted to fabricate the devices [6]. The first step in the methodology for the design of the device in this simulation environment is the selection of appropriate materials. The physical and mechanical properties of interest in this case are the Young's modulus of elasticity, density and the electrical conductivity of the materials. The device is fabricated by first depositing a silicon dioxide ( $\text{SiO}_2$ ) insulating layer on a silicon (Si) substrate. This is followed by the deposition of the aluminium (Al) conducting layer on the  $\text{SiO}_2$  layer. The Al and  $\text{SiO}_2$  layers are patterned by photoresist photolithography to leave a U-shaped structure anchored at its arms ends to the  $\text{SiO}_2$  insulating layer on the silicon substrate. As a post processing micromachining step, the back side of the silicon substrate is anisotropically etched to release the cantilever structure from the substrate. Several U-shaped Al cantilevers of various thicknesses (from 1  $\mu\text{m}$  to 20  $\mu\text{m}$ ) and various widths (from 5  $\mu\text{m}$  to 20  $\mu\text{m}$ ) were designed with the lengths of the arms and the base kept constant at 1000  $\mu\text{m}$  and 760  $\mu\text{m}$ , respectively. Fig. 3 shows an example of the 3D solid models of the devices generated by the software while Fig. 4 shows the backside of the silicon substrate layer that has been anisotropically etched to release the U-shaped cantilever.

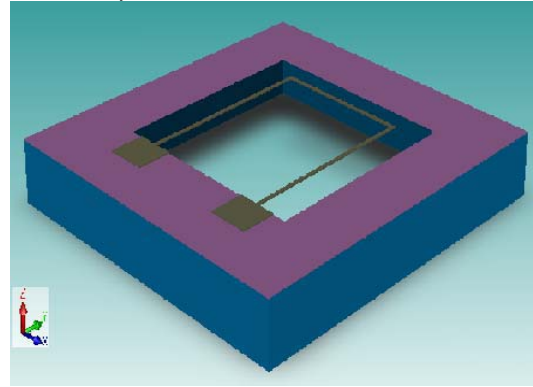


Fig. 3. 3D solid model of the U-shaped cantilever device

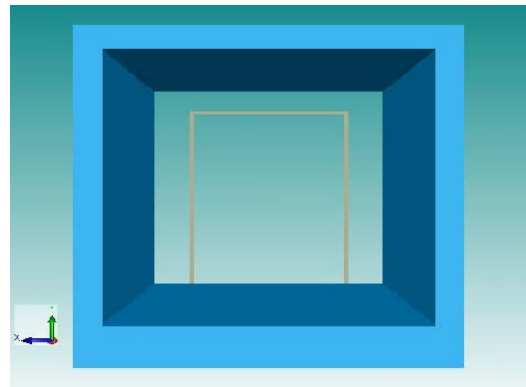


Fig. 4. Anisotropic back side etching of the U-shaped cantilever device

In order to simulate the cantilever response under applied Lorentz forces, two methods of characterization are used; static and dynamic. The static characterization is realized by applying a constant force to the base or arms of the cantilever corresponding to the macroscopic forces on sections of the U-shaped cantilever generated by the action of the Lorentz force. For dynamic characterization, a periodic force of the same amplitude as the static is applied to both the base and the arms for harmonic analysis. This periodic force is applied in such a way as to generate one of the three flexural vibration modes shown in Fig. 1 (b). The appropriate Lorentz force is calculated using (1) by considering a current of 10 mA, an external static magnetic field of 9 mT and length  $l$  of arm of 1000  $\mu\text{m}$  to give a value of 1.2  $\mu\text{N}$  for the force on the arms and taking the length of base of 760  $\mu\text{m}$  to give a force of 0.9  $\mu\text{N}$  for the base.

### IV. RESULTS AND DISCUSSION

#### A. Static Characterization

In the static mode, a constant force of 1.2  $\mu\text{N}$  or 0.9  $\mu\text{N}$  is applied perpendicular to the arms or base, respectively, representing the Lorentz force due to a constant dc current in a static magnetic field that is perpendicular to the arms or base. Fig. 5 shows a maximum displacement of 9.1  $\mu\text{m}$  on the base when the constant force is applied on the base in the  $-ve$   $z$ -direction. Fig. 6 shows a maximum displacement of about 2.0  $\mu\text{m}$  at the extremity of both arms in the  $z$ -direction when

the force is applied in opposite direction on each arm. Fig. 7 shows a maximum inward displacement of 3.6 nm at the centre of each arm in  $y$ -direction while a negligible displacement in the  $x$ -direction at the base is observed for a static magnetic field perpendicular to both the arms and the base. The base experiences a slight outwards net displacement because the inward acting Lorentz force is slightly less than the outward mechanical force that is induced on the base when an inward force is applied to both the arms simultaneously.

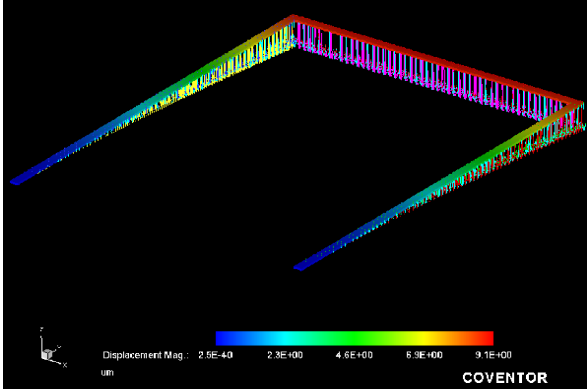


Fig. 5: Vector displacement of a constant downward force of  $0.9 \mu\text{N}$  applied to the base

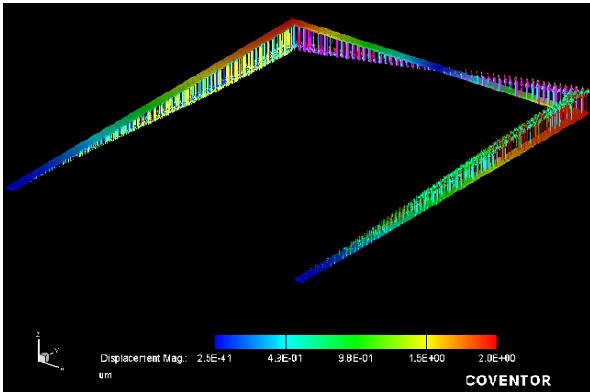


Fig. 6: Vector displacement of a constant force of  $1.2 \mu\text{N}$  applied to the arms in opposite direction

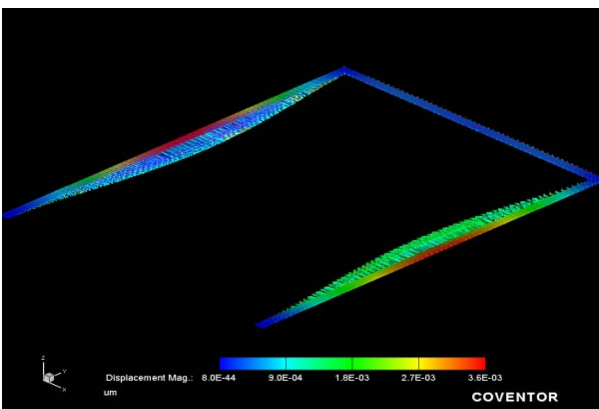


Fig. 7: Vector displacement of a constant inward force of  $1.2 \mu\text{N}$  and  $0.9 \mu\text{N}$  applied to the arms and base, respectively

The frequency response of the various modes are obtained by a frequency sweep, in the resonance neighbourhoods of the theoretically calculated values, for thicknesses and widths of 5, 10 and 15  $\mu\text{m}$  to obtain the dynamic characteristics when a periodic (sinusoidal) force of amplitude  $1.2 \mu\text{N}$  for the arms, and  $0.9 \mu\text{N}$  for the base, is applied. The resonant frequency is determined from the graphs of displacement as a function of frequency. Figs. 8, 9 and 10 show the effect of cantilever thickness on its displacement profile for modes 1, 2 and 3, respectively, while Figs. 11, 12 and 13 show the effect of width on its displacement profile for modes 1, 2 and 3, respectively. Figs. 8 and 9 show that the resonant frequencies for modes 1 and 2 are significantly influenced by thickness with the resonant frequency increasing with increasing thickness while the displacement amplitude at resonance decreases. Fig. 10, however, shows that the resonant frequency and amplitude are independent of thickness for mode 3. It is observed from Figs. 8 to 10 that the displacement amplitude at resonance is highest, indicating highest sensitivity, for mode 1 followed by mode two and lowest for mode 3.

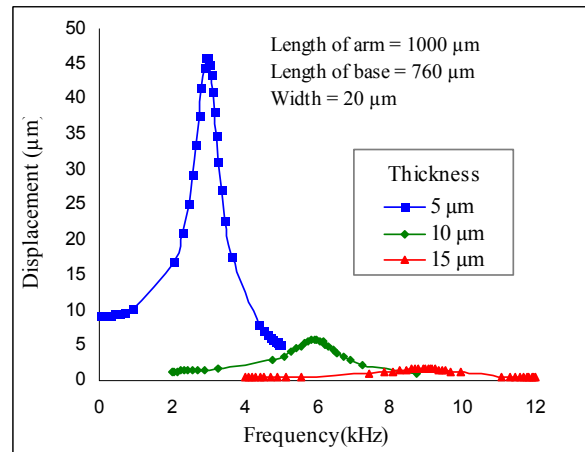


Fig. 8. Displacement of the U-shaped cantilever vs frequency at different thickness for mode 1

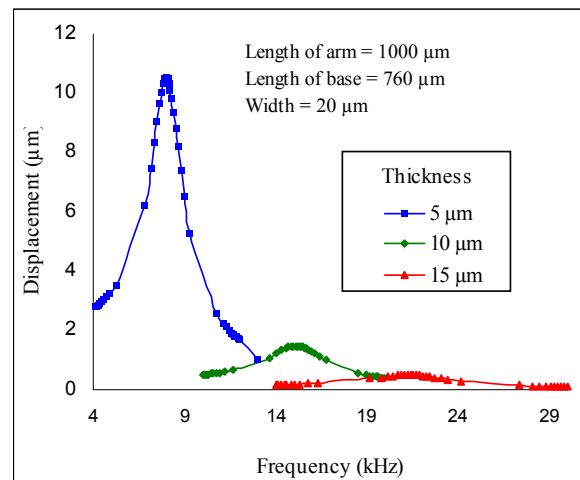


Fig. 9. Displacement of the U-shaped cantilever vs frequency at different thickness for mode 2

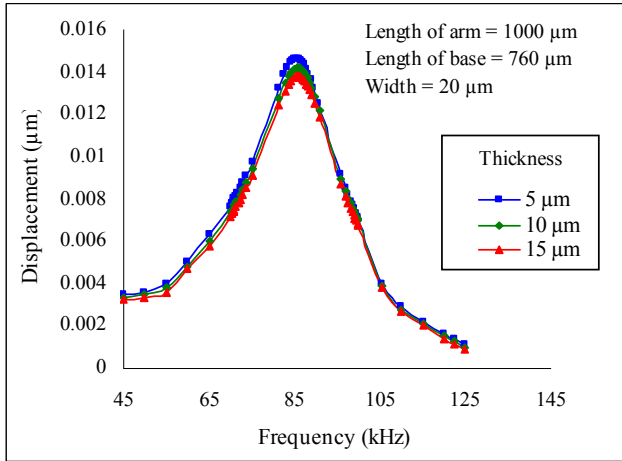


Fig. 10. Displacement of the U-shaped cantilever vs frequency at different thickness for mode 3

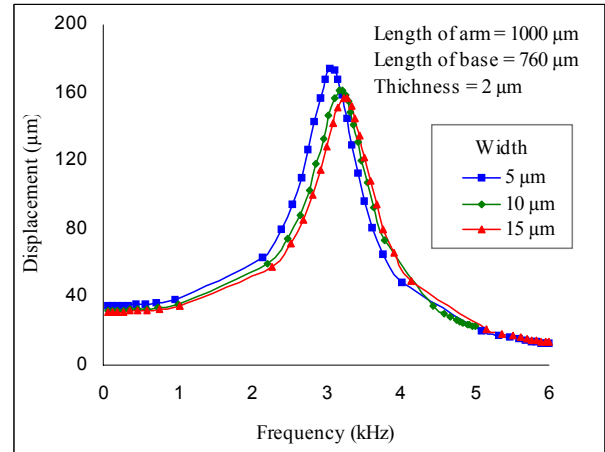


Fig. 12: Displacement of the U-shaped cantilever vs frequency at different widths for mode 2

On the other hand, Figs. 11 and 12 shows that the resonant frequencies and displacement amplitudes for modes 1 and 2 are independent of the width of the U-shaped cantilever. However, for mode 3 as shown in Fig. 13, the resonant frequency increases with increasing width while the displacement amplitude at resonance decreases. In general, therefore, simulation results indicate that the displacement of the cantilever is significantly larger when a periodic force is applied at its natural frequency (resonant frequency) compared to a constant force for the three modes. The results are in good agreement with the theoretically calculated values for the three modes of vibration. The resonant frequencies for the three modes of vibrations theoretically calculated are highest for mode 3, and lowest for mode 1. It is also observed from Figs. 10 to 12 that the displacement amplitude at resonance is highest, indicating again highest sensitivity, for mode 1 followed by mode two and lowest for mode 3.

Fig. 13, 14 and 15 show the theoretical and simulated values of the resonant frequencies as a function of thickness (Fig. 13) and width (Figs. 14 and 15). In all cases we observe good agreement between simulated and calculated values.

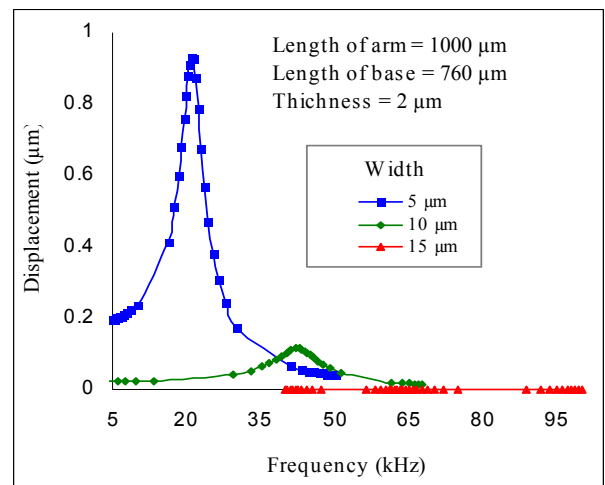


Fig. 13: Displacement of the U-shaped cantilever vs frequency at different widths for mode 3

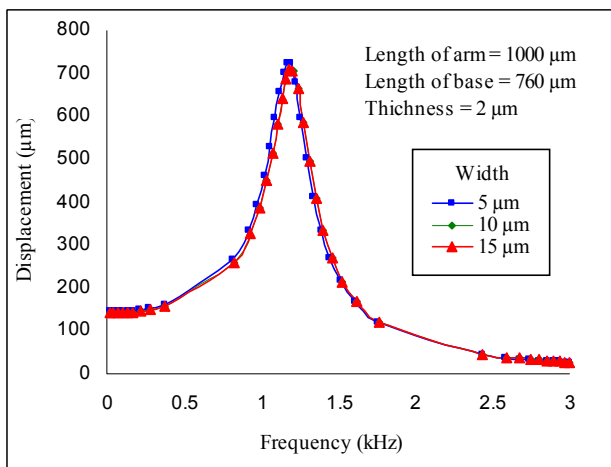


Fig. 11: Displacement of the U-shaped cantilever vs frequency at different widths for mode 1

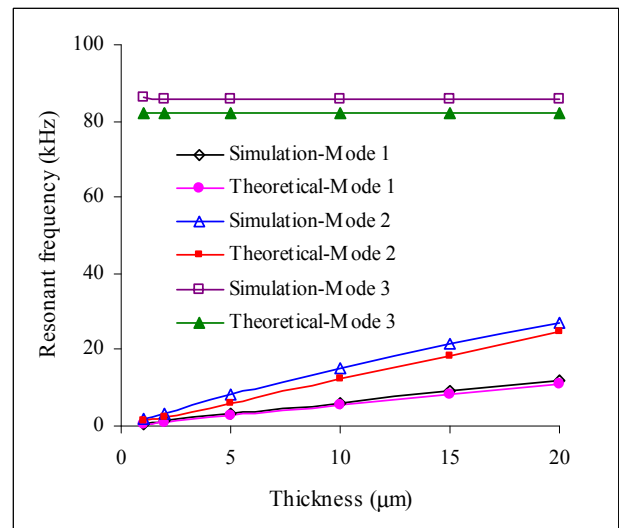


Fig. 13: Comparison of theoretical and simulation results of Resonant frequency vs thickness for the three modes of vibrations

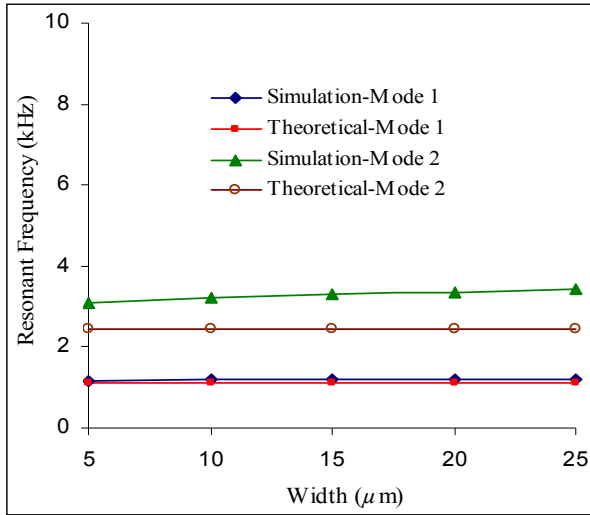


Fig. 14: Resonant frequency vs cantilever width for mode 1 and mode 2

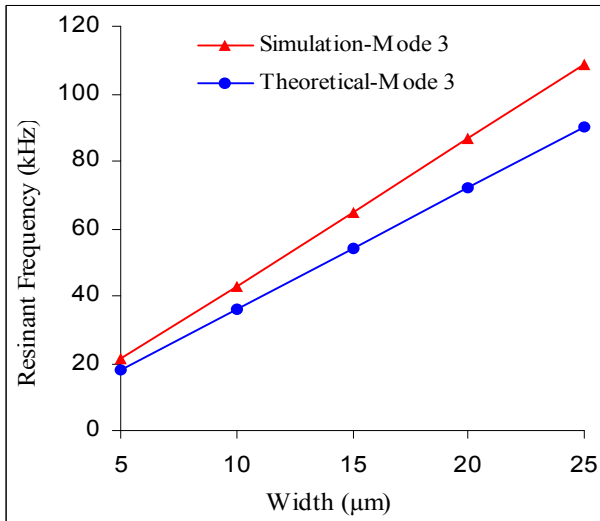


Figure 15: Resonant frequency vs cantilever width for modes 3

Analytical models describing 3-D vibration modes for U-shaped cantilever devices that are actuated by the Lorentz force and their verification by simulation is discussed. It is shown that when the cantilever is driven at or near its natural frequency by a periodic force, a large displacement is realized as compared to a static force for the three vibration modes. This high response of the device in the dynamic mode is useful for increasing sensitivity in measurement of an external magnetic field. Results also show that the resonant frequencies are directly proportional to the thickness of the cantilevers for mode 1 and 2 while it is independent of the thickness for mode 3. However unlike mode 1 and 2, the resonant frequency in mode 3 is significantly influenced by the variations in the width of the U-shaped cantilever. The theoretically calculated values for the resonant frequencies in all modes agree quite well with the simulation results.

#### REFERENCES

- [1] N. Dumas, L. Latorre, P. Nouet "Low noise CMOS amplifier for a piezoresistive magnetic field sensor", *18th Conference on Design of Circuits and Integrated Systems (DCIS'03)*, Ciudad Real, Spain, 19-21 November 2003, p. 639-644.
- [2] El Mehdi, Yannick S, Frederick M, Laurent L and Pascal, "Rejection of Power Supply Noise in Wheatstone Bridges Application to Piezoresistive MEMS", *Proc. of DTIP of MEMS & MOEMS*, 2008.
- [3] Vincent B, Yves B, Laurent L, Pascal N, "Monolithic piezoresistive CMOS magnetic field sensors" *Sensors and Actuators A*, vol 103, 2003, pp32-23.
- [4] F. Keplinger, R. Beigelbeck, F. Kohl, "Simultaneous Measurement of Two Magnetic Field Components Using a U-Shaped Cantilever Device", *3rd IEEE Conference on Sensors*, 2004, pp1450-1453.
- [5] Franz Keplinger et al., "Frequency and Transient Analysis of Micromachined U-shaped Cantilever Devices for Magnetic Field Measurement" *13th International Conference on Solid State Sensors, Actuators and Microsystems*, Seoul, Korea, 2005.
- [6] M. Elwensspöck, R. Wiegand, *Mechanical microsensors*, Springer, Singapore, 2001.